

Published in final edited form as:

Sci Signal. ; 3(125): ra45. doi:10.1126/scisignal.2000549.

Purinergic Signaling: A Fundamental Mechanism in Neutrophil Activation

Yu Chen, Yongli Yao, Yuka Sumi, Andrew Li, Uyen Kim To, Abdallah Elkhail, Yoshiaki Inoue, Tobias Woehrle, Qin Zhang, Carl Hauser, and Wolfgang G. Junger*

Department of Surgery, Beth Israel Deaconess Medical Center, Harvard Medical School, Boston, MA 02215, USA

Abstract

Efficient activation of neutrophils is a key requirement for effective immune responses. We found that neutrophils released cellular adenosine triphosphate (ATP) in response to exogenous stimuli such as formylated bacterial peptides and inflammatory mediators that activated receptors for Fc γ , interleukin-8, C5a complement, and leukotriene B₄. The release of ATP in response to stimulation of the formyl peptide receptor (FPR) occurred through pannexin-1 hemichannels that colocalized with FPR and P2Y₂ nucleotide receptors on the cell surface to form a purinergic signaling system that facilitated the activation of neutrophils. Disruption of this purinergic signaling system by inhibiting or silencing pannexin-1 hemichannels or P2Y₂ receptors blocked the activation of neutrophils and impaired innate host responses to bacterial infection. Thus, purinergic signaling is a fundamental mechanism that is required for neutrophil activation and immune defense.

Introduction

Polymorphonuclear neutrophils (PMNs) form the first line of defense against invading pathogens; however, in addition to their beneficial actions in host defense, neutrophils are also involved in pathophysiological processes that lead to damage of host tissue in inflammatory diseases, sepsis, and ischemia-reperfusion injury after severe trauma and hemorrhage (1). Migration, degranulation, and the respiratory burst are key functional responses that enable PMNs to accomplish their tasks in host defense. These functional responses are triggered by receptors that recognize bacterial peptides such as N-formyl-

*Corresponding author. wjunger@bidmc.harvard.edu.

Author contributions: Y.C. performed most experiments and prepared the manuscript and figures; Y.Y. and U.K.T. provided technical and logistical assistance. Y.S., T.W., Y.L., and A.E. performed the animal experiments. A.L. and Q.Z. performed calcium measurements and C.H. helped with the discussion and interpretation of results. W.G.J. was responsible for the design and coordination of the study and he finalized the manuscript.

Conflicts of interest: The authors have no conflicts of interest to declare.

Supplementary Materials

Fig. S1. Colocalization of FPR (green) and TTYH3 (red) in polarized human PMN.

Fig. S2. Effect of ATP release blockers on the ability of PMN to hydrolyze extracellular ATP.

Fig. S3. Effect of ATP release blockers on ATP-induced Ca²⁺ mobilization.

Fig. S4. Silencing of P2Y₂ receptors and TTYH3 channels.

Fig. S5. Colocalization of P2Y₂ receptors and FPR.

Movie S1. Z-stack view of a dHL-60 cell co-transfected with P2Y₂-ECFP (green) and FPR-EYFP (red).

Movie S2. The 3D view of a dHL-60 cell co-transfected with P2Y₂-ECFP (green) and FPR-EYFP (red).

methionyl-leucyl-phenylalanine (fMLP) or innate inflammatory mediators such as interleukin-8 (IL-8), leukotriene B₄ (LTB₄), and the complement product C5a, which orchestrate the responses of PMNs during inflammation and host defense (2–4). Similar to the formyl peptide receptors (FPRs), all of these PMN receptors belong to the G protein–coupled receptor (GPCR) superfamily, which use heterotrimeric guanine nucleotide binding proteins (G proteins) to trigger downstream processes, including mobilization of calcium ions (Ca²⁺) and mitogen-activated protein kinase (MAPK) signaling, which induce functional cell responses. However, other receptors that are unrelated to GPCRs, such as the Fcγ receptors (FcγRs) also play critical roles in host defense by eliciting the phagocytosis and killing of invading bacteria.

Intracellular adenosine triphosphate (ATP) serves as a source of energy that drives virtually all cell functions; however, when released into the extracellular space, ATP serves as an intercellular messenger or an autocrine mediator that regulates cell functions. Through paracrine and autocrine mechanisms and the activation of purinergic receptors, ATP and its metabolites, including adenosine, modulate the biological functions of mammalian cells (5–9). Purinergic receptors are separated into two families: P1 adenosine receptors and P2 nucleotide receptors, which are further divided into the P2X and P2Y receptor subfamilies. P2X receptors consists of seven members that function as ATP-gated ion channels and the P2Y receptor family is comprised of eight members that are GPCRs and recognize ATP, UTP, and related molecules (9–11). We previously found that extracellular ATP controls chemotaxis of PMNs through P2Y2 receptors (12). Here, we show that ATP is released by pannexin-1 hemichannels and that autocrine feedback through P2Y2 receptors is an essential purinergic signaling mechanism that is required for the activation of PMNs by a wide range of extracellular stimuli and that regulates the responses of PMNs in immune defense and inflammation.

Results

Stimulation of FPR triggers the release of ATP through maxi-anion channels and pannexin-1 hemichannels

Stimulation of FPR causes the rapid release of ATP from PMNs (12). Mammalian cells can release cellular ATP through various mechanisms. Among these, release through connexin and pannexin hemichannels and maxi-anion channels have been observed in different cell types (13–16). The human tweety homolog 1 (hTTYH1) and hTTYH3, which encode maxi-anion channels, are human homologues of a gene located in *Drosophila* flightless and are expressed in human leukocytes (15). Maxi-anion channels are associated with large-conductance chloride currents and can facilitate the release of ATP from mammalian cells (17). The various pannexin (Panx) and connexin (Cx) gap-junction proteins form hemichannels that release ATP from leukocytes (14, 16). Cx43 hemichannels facilitate the release of ATP from PMNs, whereas Panx 1 hemichannels are involved in the release of ATP from T lymphocytes (14, 16). Through real-time, reverse transcriptase polymerase chain reaction (RT-PCR) analysis, we found that human PMNs, undifferentiated neutrophil-like HL-60 cells, and differentiated HL-60 cells (dHL60) expressed the genes encoding TTYH3 and Panx 1, but not those encoding TTYH1 or Cx43 (Fig. 1A). Consistent with

these data, immune cytochemistry experiments revealed that human PMNs contained TTYH3 and Panx 1, but neither TTYH1 nor Cx 43 (Fig. 1, B and C). We found that fMLP induced the translocation of Panx 1 to the leading edge in $80 \pm 16\%$ of polarized PMNs, which was identified by staining of the F-actin-rich leading edge of the cells with phalloidin (Fig. 1, C and D). Staining of cells with antibodies against Panx 1 and FPR revealed that Panx 1 colocalized extensively with FPR at the leading edge of polarized PMNs, where the greatest extent of F-actin staining was observed (Fig. 1D). By contrast, TTYH3 channels colocalized with FPR only in segregated foci that remained more uniformly distributed across the cell surface (fig. S1).

Panx 1 and TTYH3 are sensitive to the anion channel inhibitor 4,4'-diisothiocyanostilbene-2,2'-disulfonic acid (DIDS) (15, 18). We found that DIDS dose-dependently blocked fMLP-induced release of ATP and functional cell responses, including production of the adhesion molecule CD11b, migration of PMNs, and oxidative burst (Fig. 2). These results indicated that the stimulation of PMN responses by FPR required the release of cellular ATP through DIDS-sensitive Panx 1 or TTYH3 channels. The effectiveness with which DIDS inhibited the various cell functions varied, with half-maximal suppression of the production of CD11b, migration, and oxidative burst at DIDS concentrations of 5, 30, and 50 μM , respectively. This suggested that different functional responses differed with regard to their requirements for purinergic signaling and the involvement of ATP or adenosine, which is formed by ecto-nucleotidases that could also be affected by DIDS (fig. S2) (19, 20).

To further evaluate the role of pannexin hemichannels, we used carbenoxolone (CBX), a more specific inhibitor of gap junction channels (18), and $^{10}\text{Panx 1}$, a mimetic blocking peptide that selectively inhibits Panx 1 hemichannels (16, 21). CBX dose-dependently suppressed fMLP-induced ATP release and functional PMN responses (Fig. 2, B and D). In contrast to DIDS, CBX did not affect ecto-nucleotidase activity or the ability of PMNs to hydrolyze extracellular ATP (fig. S2). $^{10}\text{Panx 1}$ reduced FPR-induced ATP release and functional responses, whereas a control peptide (23) had little effect on these responses (Fig. 2, B and E). Whereas knockdown of TTYH3 with siRNA reduced FPR-induced ATP release by 70% compared to that in control cells, the oxidative burst of HL-60 cells was only marginally affected (Fig. 2F). These results showed that TTYH3 and pannexin hemichannels both facilitated the release of ATP but that only Panx 1-mediated release of ATP seemed to play a role in FPR-induced functional responses. Treatment of PMNs with $^{10}\text{Panx 1}$, DIDS, or CBX reduced FPR-induced release of ATP by no more than 80%, which suggested that the remaining 20% was mediated by unrelated mechanisms. However, knockdown of TTYH3 channels in dHL-60 cells blocked the release of ATP by 70% relative to that of control cells, which indicated that there were either complex interactions between Panx 1- and TTYH3-induced ATP release or differences between PMNs and dHL-60 cells with regard to the contributions of these two channels to the release of ATP.

Extracellular ATP and P2Y2 receptors are required for FPR-induced activation of PMNs

Enzymes that hydrolyze extracellular ATP block the migration of PMNs (12). This observation and our data indicated that the release of ATP and autocrine feedback through

ATP receptors were essential steps that linked the stimulation of FPRs with subsequent functional responses of PMNs. To study how released ATP influenced downstream signaling events triggered by FPR, we assessed intracellular Ca^{2+} mobilization in PMNs that were loaded with the intracellular Ca^{2+} probe Fura-2 AM. We found that inhibition of ATP release with CBX or $^{10}\text{Panx 1}$ or elimination of released ATP with apyrase dose-dependently inhibited FPR-induced Ca^{2+} mobilization in PMNs, whereas a control peptide (23) had little effect on Ca^{2+} responses (Fig. 3A). Furthermore, CBX and $^{10}\text{Panx 1}$ did not affect ATP-induced Ca^{2+} mobilization, indicating that these inhibitors blocked the FPR-induced release of ATP and did not directly affect P2 receptor-induced Ca^{2+} mobilization (fig. S3). Compared to CBX or $^{10}\text{Panx 1}$, relatively high concentrations of apyrase (5 to 20 U/ml) were needed to suppress the mobilization of Ca^{2+} . This suggested that apyrase was less potent than CBX and $^{10}\text{Panx 1}$ in blocking purinergic signaling, because apyrase must compete with purinergic receptors for released ATP, whereas CBX and $^{10}\text{Panx 1}$ inhibit the upstream release of ATP and thus more effectively intercept purinergic signaling in response to the stimulation of FPRs. However, we observed that CBX and $^{10}\text{Panx 1}$ did not completely block Ca^{2+} mobilization, which suggested that Ca^{2+} mobilization depended on both purinergic signaling and direct FPR-induced pathways that were independent of purinergic receptors.

Next, we tested whether the release of ATP was required for FPR-induced activation of extracellular signal-regulated kinase (ERK). CBX and apyrase dose-dependently reduced the activation of ERK (Fig. 3B). This indicated that ERK activation, like Ca^{2+} signaling, depended on the release of ATP. We used the P2 receptor antagonist suramin to evaluate the role of purinergic receptors in FPR-induced cell signaling and functional PMN responses. Suramin dose-dependently reduced degranulation, oxidative burst, and chemotaxis as well as the activation of ERK and the mobilization of Ca^{2+} (Fig. 4, A to C), indicating that P2 receptors were indispensable for the activation of PMNs. P2Y2 receptors are the most abundant P2 receptor subtype in human PMNs and dHL-60 cells (12). We found that knockdown of P2Y2 receptors, which reduced the abundance of P2Y2 mRNA by >80% in dHL-60 cells (fig. S4A), markedly inhibited FPR-induced Ca^{2+} mobilization and oxidative burst (Fig. 4, D and E). Thus, P2Y2 receptors were central to the activation of PMNs in response to stimulation of FPRs.

FPR and P2Y2 receptors colocalize on the surface of PMNs

Rapid responses of the purinergic signaling systems described earlier require the close proximity of FPR, Panx 1, and P2Y2 receptors to effectively convey extracellular cues to functional responses. As shown earlier, Panx 1 colocalizes with FPR (Fig. 1D). We examined whether P2Y2 receptors also colocalized with FPR by cotransfecting dHL-60 cells with plasmids encoding P2Y2 tagged with enhanced cyan fluorescent protein (ECFP) and FPR tagged with enhanced yellow fluorescent protein (EYFP). FPR and P2Y2 indeed colocalized extensively on the surface of unstimulated dHL-60 cells (Fig. 5, and Movies S1 and S2). After stimulation with fMLP to induce polarization, P2Y2 and FPR remained colocalized and were found across the surface of dHL-60 cells; however, colocalization was not observed in some subcellular structures, suggesting that FPR and P2Y2 associated with different cytosolic granules or organelles (Fig. 5 and fig. S5). Together, our findings show

that FPR and P2Y2 form tight spatiotemporal associations that enable effective purinergic signaling and may serve to amplify FPR-induced activation signals through autocrine purinergic feedback loops.

Purinergic signaling is a fundamental activation process in PMNs

Our findings thus far indicated that signaling and functional responses to fMLP required the release of ATP and autocrine feedback through P2Y2. We tested whether similar purinergic feedback mechanisms controlled the responses of PMNs to other extracellular stimuli. FcγRs enable PMNs to recognize and phagocytose opsonized particles. We found that stimulation of FcγR also triggered the release of ATP. Similar to our findings with FPR, treatment with DIDS or CBX or inhibition of P2 receptors inhibited FcγR-induced release of ATP, formation of superoxide, and phagocytosis of opsonized bacteria (Fig. 6, A to C). Moreover, stimulation of PMNs through receptors for IL-8, C5a, and LTB₄ also induced the release of ATP, and the activation of ERK in response to these stimuli was blocked by DIDS and CBX (Fig. 6, D to F). Thus, purinergic signaling did not seem to be restricted to FPR signaling but appeared to constitute a fundamental mechanism that was involved in the activation of PMNs by infectious and inflammatory extracellular stimuli that triggered a range of GPCRs and other cell-surface receptors. The physiological importance of purinergic signaling for innate immune defense is underlined by our finding that PMNs from *P2RY2* knockout (P2Y2 KO) mice showed impaired FPR-induced cell responses, for example the externalization of CD11b on the cell surface (Fig. 7A). In addition, we found that chemotaxis of PMNs was diminished in P2Y2 KO animals compared to that in wild-type mice (24) and that P2Y2 KO mice were less capable than their wild-type counterparts to contain bacterial infections, which resulted in substantially higher bacterial counts in the peritoneal cavities and in the livers, lungs, and spleens of infected P2Y2 KO mice compared to those in wild-type, control mice (Fig. 7B).

Discussion

Whereas PMNs play an important role in protecting the host from infections, they are also responsible for tissue damage in the host that occurs in a number of inflammatory diseases, such as reperfusion injury, rheumatoid arthritis, inflammatory bowel disease, and asthma (1, 25). To devise effective therapeutic approaches that reduce PMN-induced tissue damage in these diseases, it is necessary to understand the signaling mechanisms that are involved in the activation of PMNs. In this report, we provided evidence that the release of ATP and autocrine purinergic signaling were central to the activation of PMNs. We showed that agonists of FPR and other GPCRs as well as of structurally unrelated receptors on PMNs triggered the release of ATP, which facilitated downstream signaling events that were required for the activation of functional cell responses. Purinergic signaling processes thus represent potential targets for therapeutic approaches to modulate the responses of PMNs in inflammatory or infectious diseases.

One such therapeutic approach could be to block the release of ATP. Although membrane-localized transporters, such as connexin and pannexin hemichannels, TTYH maxi-anion channels, and vesicular transport are implicated in the release of ATP from mammalian cells

(15, 17, 26–33), a clear understanding of which of these mechanisms facilitates the release of ATP from human PMNs in response to cell stimulation has been lacking. Some studies have shown that PMNs release ATP through Cx 43 hemichannels (14). Here, we showed that human PMNs released ATP through TTYH3 maxi-anion channels and Panx 1 hemichannels, which are also implicated in the release of ATP from human T cells (16). Although TTYH3 maxi-anion channels and Panx 1 hemichannels release ATP, we found that only ATP that was released from Panx 1 hemichannels facilitated the functional responses of the cells that we investigated. Thus, the blockade of Panx 1 hemichannels may be a possible strategy to intercept purinergic signaling and to inhibit the activation of PMNs in inflammatory diseases. This notion is supported by reports that CBX, an inhibitor of Panx 1, prevents allergic airway inflammation in a mouse model of asthma (34).

GPCRs can form dimeric structures or higher-order oligomeric complexes that modulate the diverse biological responses elicited by these receptors (35). In addition to homomeric structures, GPCRs can also form heterodimers with unrelated GPCRs. Heterodimerization results in agonist specificities that seem to modify receptor functions (36). A number of purinergic receptor subtypes are thought to form such heterodimers either with other purinergic receptor subtypes (for example, A1 adenosine receptors with P2Y1 receptors) or with unrelated GPCRs (for example, A2a adenosine receptors with D2 dopamine receptors) (37, 38). Our findings showed that FPR and P2Y2 colocalized closely on the surface of PMNs, suggesting that they might form heteromeric complexes that associate with Panx 1 and thus could amplify FPR-induced signaling through purinergic autocrine feedback loops.

Extracellular nucleotides, such as ATP and its hydrolytic products, and purinergic receptors regulate a number of physiological processes, such as chloride secretion of epithelial cells, the redistribution of blood flow, and neurotransmission (39). Released ATP and other nucleotides activate P2 receptors that control cell functions that are associated with these physiological processes. Several studies reported that the activation of P2Y2 is involved in the production of IL-8 by retinal pigment epithelium cells and in the clearance of apoptotic cells by phagocytes (40, 41). Here, we showed that P2Y2 proteins formed a critical link in the signaling process that resulted in the activation of PMNs by infectious or inflammatory mediators. Our findings indicate that, although such inflammatory mediators induce certain signaling responses, such as the activation of ERK, in the absence of purinergic signaling, the initiation of effective functional responses in PMNs cannot occur without the release of ATP and autocrine purinergic feedback. Thus, to respond to specific extracellular cues, PMNs require both (i) specialized receptors that detect inflammatory or infectious mediators, and (ii) purinergic receptors that define and regulate the functional responses to such mediators.

Materials and Methods

Reagents and expression constructs

Apyrase, 4,4'-diisothiocyanato-stilbene-2,2'-disulfonic acid (DIDS), carbenoxolone (CBX), human immunoglobulin G₁ (IgG₁-κ) antibodies, and dextran were from Sigma-Aldrich and 8,8'-(carbonylbis(imino-4,1-phenylenecarbonylimino-4,1-phenylenecarbonylimino))bis-1,3,5-naphthalenetrisulfonic acid (suramin) was from

Calbiochem. Percoll was obtained from Pharmacia. ¹⁰Panx 1 was from Tocris Bioscience and the Panx 1 control peptide (23) was from AnaSpec Inc. The mammalian expression vectors pEYFP-N1 and pEGFP-N1 were obtained from Clontech Laboratories. Expression vectors encoding fluorescent fusion proteins of human FPR1 and TTYH3 were generated in our laboratory from an FPR1-encoding plasmid obtained from Missouri S&T cDNA Resource Center and a hTTYH3 plasmid purchased from Thermo Fisher Scientific, Open Biosystems. All DNA constructs were confirmed by sequencing. The pECFP-P2Y2 receptor construct was a kind gift from Drs. Harald Sitte and Christian Nanoff, Medical University of Vienna, Vienna, Austria.

Isolation and treatment of human PMNs

All studies were approved by the Institutional Review Board of the Beth Israel Deaconess Medical Center. PMNs were isolated from the peripheral blood of healthy volunteers as described previously (42). Before stimulation, PMNs were pretreated with different concentrations of DIDS, suramin, ¹⁰Panx 1, or apyrase for 10 min, unless indicated otherwise. These treatments did not change the viability of PMNs as determined by trypan blue dye exclusion.

Chemotaxis assays and measurements of MAPK activity

Chemotaxis assays and assays of the activity of MAPKs were performed as described previously (12, 42). PMNs were stimulated with 100 nM fMLP for 1 min in the case of MAPK assays or with 1 nM fMLP for 50 min for chemotaxis assays and functional cell responses were determined.

Immunofluorescence staining

Human PMNs (2.5×10^6 /ml) were plated on flamed 25-mm glass coverslips for 10 min at room temperature. All subsequent steps were performed at room temperature. The cells were fixed for 15 min with 3.7% paraformaldehyde in Hank's balanced salt solution (HBSS, Irvine Scientific). After rinsing with HBSS, cells were permeabilized for 1 min with HBSS containing 0.01% Triton X-100 and blocked for 60 min with 5% human serum. The cells were incubated for 1 hour with rabbit antibody against human TTYH3 (1:200), goat antibody against human Panx 1 (1:200), or mouse antibody against human FPR (1:200). Cells were then incubated for 30 min in the dark with the appropriate secondary antibodies (1:1000): Alexa Fluor-555–conjugated goat antibody against rabbit IgG for hTTYH3, Alexa Fluor-594–conjugated rabbit antibody against goat IgG for Panx 1, and Alexa Fluor-488–conjugated goat antibody against mouse IgG for FPR. F-actin was stained with phalloidin (5 U per slide, Invitrogen). Fluorescence and bright field images were acquired with a Leica DM-IRB fluorescence microscope. Control cells were treated identically except that incubation with primary antibodies was omitted. The presence of TTYH1 and Cx 43 in human PMNs was examined by staining with rabbit antibody against human TTYH1 (1:200) or with rabbit antibody against human Cx 43 (1:200). Antibody against human Cx 43 were purchased from Cell Signaling Technology and antibodies against human TTYH1 and TTYH3 were generous gifts of Dr. Suzuki (Jichi Medical School, Tochigi, Japan), who has demonstrated that these antibodies only recognize the respective human TTYH protein isoforms (15). Antibody against FPR was from BD Pharmingen and antibody against Panx 1

was from Santa Cruz Biotechnology, and the selectivities of these antibodies were verified by their manufacturers.

Phagocytosis assays

An Alexa Fluor-488-labeled preparation of *Escherichia coli* was purchased from Invitrogen. Bacteria were opsonized by incubating equal volumes of 10% human serum and 20 mg/ml of suspended bacteria for 1 hour at 37°C. After 2 washes in HBSS, bacteria were incubated with PMNs at a ratio of 10:1 at 37°C for 30 min. Reactions were stopped by adding ice-cold 1% formaldehyde in HBSS, and the cells were washed with 1% formaldehyde in HBSS. Uptake of bacteria was analyzed by flow cytometry according to the manufacturer's guidelines.

Oxidative burst and degranulation assays

Oxidative burst was measured with dihydrorhodamine 123 (DHR; Invitrogen). Isolated PMNs were incubated with DHR (100 μ M) and fMLP (100 nM) for 20 min and then placed on ice for 10 min to stop the reactions. Degranulation of PMNs was assessed by measuring the abundance of CD11b on the cell surface. PMNs were stimulated with fMLP (100 nM) for 10 min, chilled on ice, stained for 20 min each with monoclonal antibodies against CD11b/Mac-1 (BD Pharmingen) and phycoerythrin (PE)-conjugated horse antibody against mouse IgG (Sigma). Oxidative burst and degranulation were analyzed by flow cytometry with a BD FacsCalibur flow cytometer (Becton Dickinson). To assess the abundance of CD11b on the surface of mouse PMNs, 100 μ l of mouse whole blood was diluted with 100 μ l of HBSS, incubated for 20 min on ice and in the dark with fluorescein isothiocyanate (FITC)-conjugated antibody against CD11b and PE-conjugated antibody against Gr-1 (both from Invitrogen and used at 1:200 dilutions). Red blood cells were lysed for 4 min on ice with RBC Lysis Buffer (eBioscience) and the remaining cells were washed twice with HBSS, fixed with sheath fluid containing 0.5% formaldehyde, and analyzed by flow cytometry.

Cell culture and transfections

HL-60 cells were maintained and transfected with the pECFP-P2Y2 and pEYFP-FPR plasmids by electroporation as described previously (12). Briefly, cells were electroporated with 20 μ g of plasmid per 2×10^6 cells with an Eppendorf Multiporator system set to 780 V, 300 μ s, and 1 pulse or with 0.5 μ g of plasmid per 5×10^5 cells with a Neon Transfection system (Invitrogen) set to 1350 V, 35 ms, and 1 pulse, according to the manufacturers' protocols.

Measurement of ATP

Freshly isolated PMNs (2×10^6 /ml) were treated with different concentrations of DIDS or 10 Panx 1 for 10 min, stimulated with fMLP (100 nM) for 3 min or with human IgG₁ for 10 min, placed on ice, and centrifuged at 325g for 1 min in the cold. The supernatants were treated as previously described (12) and the release of ATP was evaluated by measuring the concentrations of ATP in the supernatants with an ATP Bioluminescence Assay HS II Kit

(Roche) and a Luminoskan plate luminometer (Labsystems) according to the manufacturers' instructions or by HPLC as previously described (12).

Real-time RT-PCR

The relative abundance of mRNAs for hTTYH1, hTTYH3, Cx 43, and Panx 1 in human PMNs, undifferentiated HL-60 cells, and HL-60 cells differentiated for 3 days with 1.3% DMSO (dHL-60 cells) were determined by real-time RT-PCR analysis, as described previously (12) except that an Eppendorf Mastercycler Realplex real-time PCR system was used. Human brain complementary DNA (cDNA, BioChain Inc) was used as a positive control. Predesigned QuantiTect primers were purchased from Qiagen. The supplier validated the primer sets bioinformatically and optimized them for use in real-time RT-PCR assays with SYBR Green. After performing real-time PCR analysis, we verified the correct PCR product sizes by agarose gel electrophoresis. The comparative Ct method was used for the relative quantification of gene expression as describe previously (12). The abundance of each mRNA was normalized against that of β -actin.

Confocal microscopy

The presence of fluorescently labeled receptors in HL-60 cells was examined 24 hours after electroporation. Cells (2.5×10^6 /ml) were plated on 25-mm glass bottom dishes (MatTek) coated with human fibronectin (50 μ g/ml; Sigma) and ECFP- and EYFP-labeled P2Y2 and FPR fusion proteins were imaged with a Zeiss LSM 510 Meta confocal microscope configured to excite both fluorescent proteins with multi-track mode with the 458 nm and the 514 nm laser lines of an argon laser source. The images in fig. S4 were recorded with an Ultraview VoX spinning disk confocal system from PerkinElmer with solid state diode laser sources emitting light at 442 nm and 515 nm.

Measurement of intracellular Ca^{2+}

PMNs or HL-60 cells were loaded according to the manufacturer's instructions with Fura-2-AM or Fluo-3-AM, respectively (Molecular Probes). Cells were stimulated with fMLP (10 nM). Changes in intracellular Ca^{2+} concentrations of cells loaded with Fura-2 were measured with a Kontron SFM 25 spectrofluorometer (Kontron Instruments). Ca^{2+} mobilization in HL-60 cells loaded according to the manufacturer's suggestions with Fluo-3 in the presence of Pluronic (Molecular Probes) was analyzed by flow cytometry. HL-60 cells were gated to exclude debris or cell aggregates from the analysis. Cell responses were normalized with ionomycin (5 μ M) to account for differences in the loading of Fluo-3 between individual cell preparations. Data were expressed as the percentage of the maximal Ca^{2+} response to that of the ionomycin-treated control.

Knockdown of P2Y2 and TTYH3

Six different short inhibitory RNA (siRNA) constructs (Ambion) that targeted P2Y2 (siRNA IDs: 4419, 143690, 4237, 143692, 143691, and 4331) and three different siRNA constructs (Invitrogen) that targeted TTYH3 (Cat#: HSS129677, HSS129678, and HSS129679) were tested. An unlabelled nonsense siRNA (Qiagen) was used as a negative control. The knockdown efficiency of each siRNA was initially tested in human embryonic kidney

(HEK) 293 cells (ATCC) that were cotransfected with siRNA constructs and EGFP-P2Y2 or EGFP-TTYH3 expression plasmids with Lipofectamine 2000 (Invitrogen) according to the manufacturer's instructions. Cells were harvested 24 hours later, and EGFP fluorescence was analyzed by flow cytometry. The siRNA constructs most effective in silencing EGFP-P2Y2 or EGFP-TTYH3 were selected (siRNA ID# 4237 from Ambion for P2Y2 and siRNA Cat# HSS129677 from Invitrogen for TTYH3). To verify the selectivity of knockdown experiments, a nonsense control siRNA construct was included in every experiment (fig. S4B). For silencing, HL-60 cells were transfected with 400 nM of each siRNA construct with the electroporation protocol and Eppendorf Multiporator system, as described earlier. Knockdown of P2Y2 or TTYH3 in HL-60 cells was assessed by determining the relative abundance of mRNAs by real-time RT-PCR, as described above.

Mouse model of infection

A mouse model of infection was established by performing cecal ligation and puncture (CLP) as described previously (5). C57BL/6J wild-type control mice were from the Jackson Laboratory and P2Y2 knockout mice were a generous gift from Dr. Richard Boucher, University of North Carolina, Chapel Hill. These animals were back-crossed to a C57BL/6J genetic background for a total of 10 generations (back-crossed animals were generously provided by Dr. Volker Vallon, UCSD, San Diego, CA). For bacterial culture experiments, animals were euthanized after 3 hours and peritoneal lavage fluid (3 ml), heparinized blood (1 ml), livers, spleens, and lungs were collected. Each organ was homogenized in a total of 1 ml of sterile normal saline and 10- μ l aliquots were plated onto trypticase soy agar plates (Becton Dickson), cultured for 24 hours at 37°C, and colonies were counted. For CD11b experiments, animals were euthanized 2 hours after CLP and blood was collected, incubated with antibody against CD11b, and analyzed by flow cytometry, as described earlier.

Statistical analysis

All values are expressed as the mean \pm standard deviation (SD). Statistical analysis was performed using unpaired Student's t-test or ANOVA for comparison of multiple groups. Differences between groups were considered statistically significant when $P < 0.05$.

Supplementary Material

Refer to Web version on PubMed Central for supplementary material.

Acknowledgments

We thank Drs. Harald Sitte and Christian Nanoff, Medical University of Vienna, Vienna, Austria for kindly providing the pECFP-P2Y2 receptor construct.

Funding: This study was supported in part by a Shock Society/Nova Nordisk research grant for Early Career Investigators (Y.C.) and by National Institute of Health grants GM-51477, GM-60475, AI-072287, AI-080582, and CDMRP Grant PR043034 (W.G.J.).

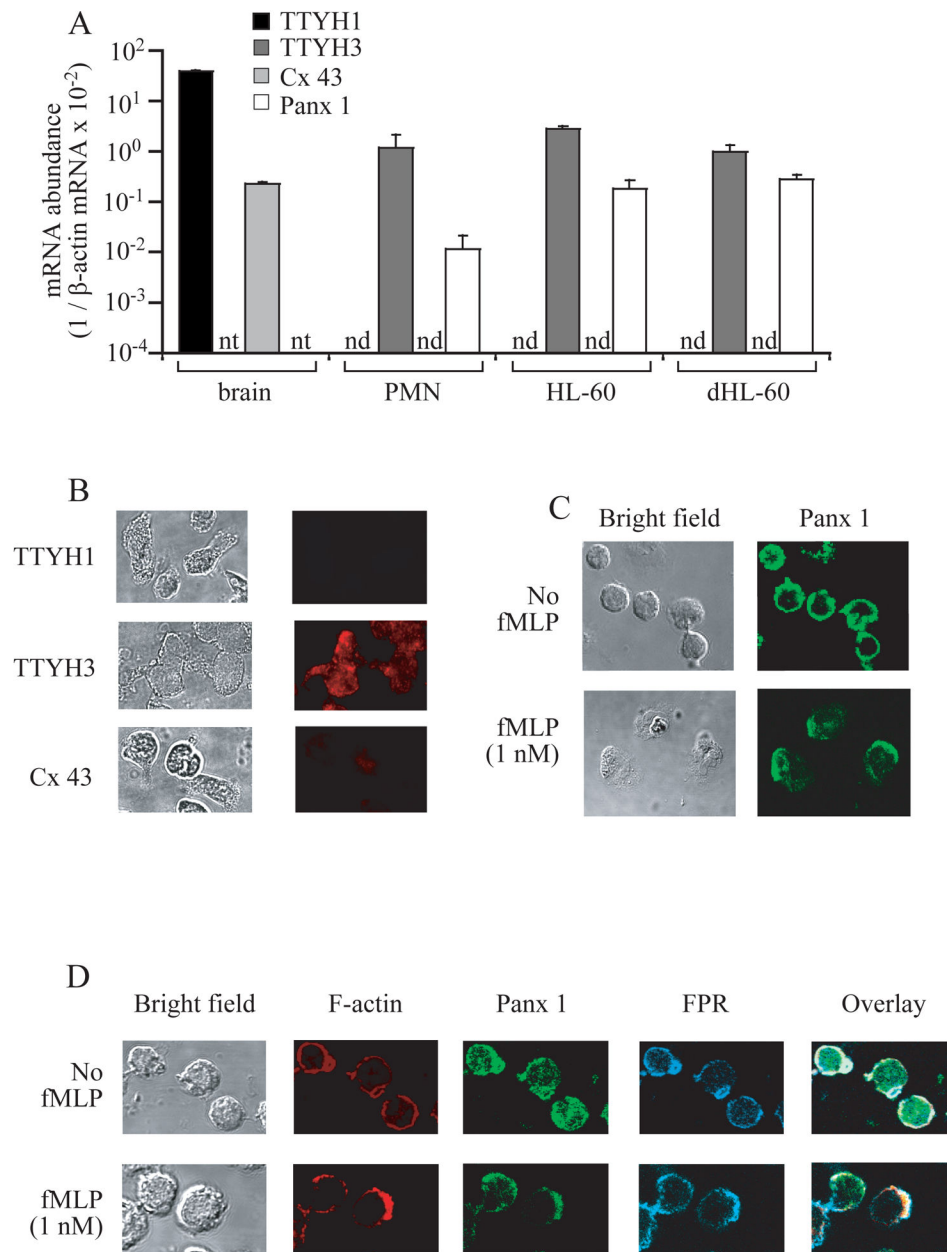
References and Notes

1. Nussler AK, Wittel UA, Nussler NC, Beger HG. Leukocytes, the Janus cells in inflammatory disease. *Langenbecks Arch Surg.* 1999; 384:222–232. [PubMed: 10328179]

2. Rabiet MJ, Huet E, Boulay F. The N-formyl peptide receptors and the anaphylatoxin C5a receptors: an overview. *Biochimie*. 2007; 89:1089–1106. [PubMed: 17428601]
3. Waugh J, Wilson C. The interleukin-8 pathway in cancer. *Clin Cancer Res*. 2008; 14:6735–6741. [PubMed: 18980965]
4. Capra V. Molecular and functional aspects of human cysteinyl leukotriene receptors. *Pharmacol Res*. 2004; 50:1–11. [PubMed: 15082024]
5. Fuller SJ, Stokes L, Skarratt KK, Gu BJ, Wiley JS. Genetics of the P2X7 receptor and human disease. *Purinergic Signal*. 2009; 5:257–262. [PubMed: 19319666]
6. Di Virgilio F, Ceruti S, Bramanti P, Abbracchio MP. Purinergic signalling in inflammation of the central nervous system. *Trends Neurosci*. 2009; 32:79–87. [PubMed: 19135728]
7. Qu Y, Ramachandra L, Mohr S, Franchi L, Harding CV, Nunez G, Dubyak GR. P2X7 receptor-stimulated secretion of MHC class II-containing exosomes requires the ASC/NLRP3 inflammasome but is independent of caspase-1. *J Immunol*. 2009; 182:5052–5062. [PubMed: 19342685]
8. Hasko G, Linden J, Crostein B, Pacher P. Adenosine receptors: therapeutic aspects for inflammatory and immune diseases. *Nat Rev Drug Discov*. 2008; 7:759–770. [PubMed: 18758473]
9. Fredholm BB. Adenosine, an endogenous distress signal, modulates tissue damage and repair. *Cell Death Differ*. 2007; 14:1315–1323. [PubMed: 17396131]
10. Burnstock G, Knight GE. Cellular distribution and functions of P2 receptor subtypes in different systems. *Int Rev Cytol*. 2004; 240:31–304.
11. Fredholm BB, IJzerman AP, Jacobson KA, Klotz KN, Linden J. International union of pharmacology. XXV. Nomenclature and classification of adenosine receptors. *Pharmacol Rev*. 2001; 53:527–552. [PubMed: 11734617]
12. Chen Y, Corriden R, Inoue Y, Yip L, Hashiguchi N, Zinkernagel A, Nizet V, Insel PA, Junger WG. ATP release guides neutrophil chemotaxis via P2Y2 and A3 receptors. *Science*. 2006; 314:1792–1795. [PubMed: 17170310]
13. Schwiebert M. ATP release mechanisms, ATP receptors and purinergic signalling along the nephron. *Clin Exp Pharmacol Physiol*. 2001; 28:340–350. [PubMed: 11339211]
14. Eltzschig K, Eckle T, Mager A, Kuper N, Karcher C, Weissmuller T, Boengler K, Schulz R, Robson SC, Colgan SP. ATP release from activated neutrophils occurs via connexin 43 and modulates adenosine-dependent endothelial cell function. *Circ Res*. 2006; 99:1100–1108. [PubMed: 17038639]
15. Suzuki M, Mizuno A. A novel human Cl(-) channel family related to Drosophila flightless locus. *J Biol Chem*. 2004; 279:22461–22468. [PubMed: 15010458]
16. Schenk U, Westendorf AM, Radaelli E, Casati A, Ferro M, Fumagalli M, Verderio C, Buer J, Scanziani E, Grassi F. Purinergic control of T cell activation by ATP released through pannexin-1 hemichannels. *Sci Signal*. 2008; 1:ra6. [PubMed: 18827222]
17. Sabirov RZ, Okada Y. ATP release via anion channels. *Purinergic Signal*. 2005; 1:311–328. [PubMed: 18404516]
18. Ma W, Hui H, Pelegrin P, Surprenant A. Pharmacological characterization of pannexin-1 currents expressed in mammalian cells. *J Pharmacol Exp Ther*. 2009; 328:409–418. [PubMed: 19023039]
19. Leite MS, Thomaz R, Oliveira JH, Oliveira PL, Meyer-Fernandes JR. Trypanosoma brucei brucei: effects of ferrous iron and heme on ecto-nucleoside triphosphate diphosphohydrolase activity. *Exp Parasitol*. 2009; 121:137–143. [PubMed: 19027737]
20. Chen Y, Hashiguchi N, Yip L, Junger WG. Hypertonic saline enhances neutrophil elastase release through activation of P2 and A3 receptors. *Am J Physiol Cell Physiol*. 2006; 290:C1051–1059. [PubMed: 16282197]
21. Pelegrin P, Surprenant A. Pannexin-1 mediates large pore formation and interleukin-1 β release by the ATP-gated P2X7 receptor. *EMBO J*. 2006; 25:5071–5082. [PubMed: 17036048]
22. Corriden R, Chen Y, Inoue Y, Beldi G, Robson SC, Insel PA, Junger WJ. Ecto-nucleoside triphosphate diphosphohydrolase 1 (E-NTPDase1/CD39) regulates neutrophil chemotaxis by hydrolyzing released ATP to adenosine. *J Biol Chem*. 2008; 283:28480–28486. [PubMed: 18713747]

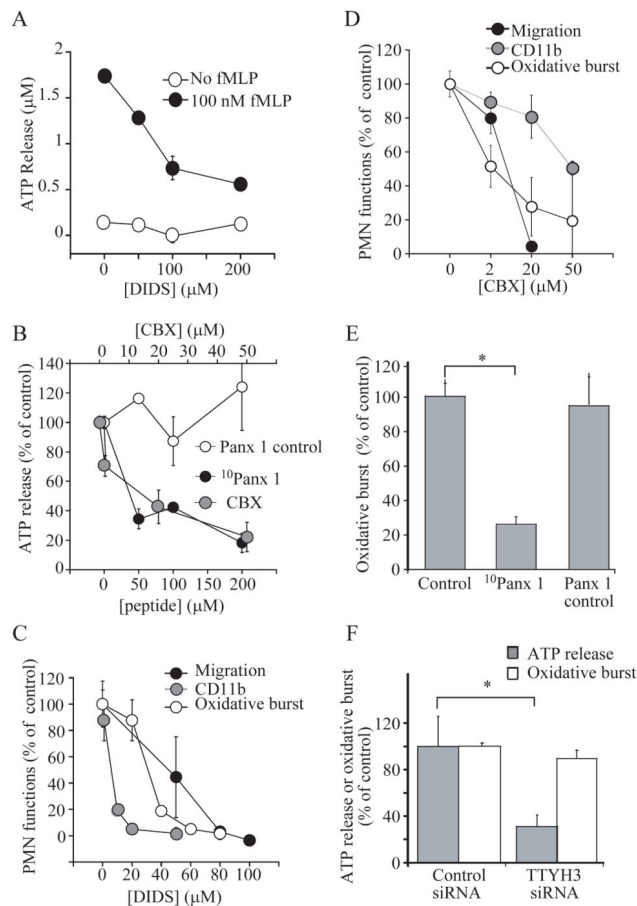
23. Thompson RJ, Jackson MF, Olah ME, Rungta RL, Hines DJ, Beazely MA, MacDonald JF, MacVicar BA. Activation of pannexin-1 hemichannels augments aberrant bursting in the hippocampus. *Science*. 2008; 322:1555–1559. [PubMed: 19056988]
24. Inoue Y, Chen Y, Hirsh MI, Yip L, Junger WG. A3 and P2Y2 receptors control the recruitment of neutrophils to the lungs in a mouse model of sepsis. *Shock*. 2008; 30:173–177. [PubMed: 18091570]
25. Weiss SJ. Tissue destruction by neutrophils. *N Engl J Med*. 1989; 320:365–376. [PubMed: 2536474]
26. Bodin P, Burnstock G. Purinergic signalling: ATP release. *Neurochem Res*. 2001; 26:959–969. [PubMed: 11699948]
27. Bao L, Locovei S, Dahl G. Pannexin membrane channels are mechanosensitive conduits for ATP. *FEBS Lett*. 2004; 572:65–68. [PubMed: 15304325]
28. Kang J, Kang N, Lovatt D, Torres A, Zhao Z, Lin J, Nedergaard M. Connexin 43 hemichannels are permeable to ATP. *J Neurosci*. 2008; 28:4702–4711. [PubMed: 18448647]
29. Bell D, Lapointe JY, Sabirov R, Hayashi S, Peti-Peterdi J, Manabe K-I, Kovacs G, Okada Y. Macula densa cell signaling involves ATP release through a maxi anion channel. *Proc Natl Acad Sci U S A*. 2003; 100:4322–4327. [PubMed: 12655045]
30. Dutta K, Sabirov RZ, Uramoto H, Okada Y. Role of ATP-conductive anion channel in ATP release from neonatal rat cardiomyocytes in ischaemic or hypoxic conditions. *J Physiol*. 2004; 559:799–812. [PubMed: 15272030]
31. Dutta K, Korchev YE, Shevchuk AI, Hayashi S, Okada Y, Sabirov RZ. Spatial distribution of maxi-anion channel on cardiomyocytes detected by smart-patch technique. *Biophys J*. 2008; 94:1646–1655. [PubMed: 18024498]
32. Sabirov Z, Dutta AK, Okada Y. Volume-dependent ATP-conductive large-conductance anion channel as a pathway for swelling-induced ATP release. *J Gen Physiol*. 2001; 118:251–266. [PubMed: 11524456]
33. Liu HT, Tashmukhamedov BA, Inoue H, Okada Y, Sabirov RZ. Roles of two types of anion channels in glutamate release from mouse astrocytes under ischemic or osmotic stress. *Glia*. 2006; 54:343–357. [PubMed: 16883573]
34. Ram A, Singh SK, Singh VP, Kumar S, Ghosh B. Inhaled carbenoxolone prevents allergic airway inflammation and airway hyperreactivity in a mouse model of asthma. *Int Arch Allergy Immunol*. 2009; 149:38–46. [PubMed: 19033731]
35. Bai M. Dimerization of G-protein-coupled receptors: roles in signal transduction. *Cell Signal*. 2004; 16:175–186. [PubMed: 14636888]
36. Franco R, Casado V, Cortes A, Mallol J, Ciruela F, Ferre S, Lluís C, Canela EI. G-protein-coupled receptor heteromers: function and ligand pharmacology. *Br J Pharmacol*. 2008; 153(Suppl 1):S90–98. [PubMed: 18037920]
37. Franco R, Ferre S, Agnati L, Torvinen M, Gines S, Hillion J, Casado V, Lledo P, Zoli M, Lluís C, Fuxe K. Evidence for adenosine/dopamine receptor interactions: indications for heteromerization. *Neuropsychopharmacology*. 2000; 23:S50–59. [PubMed: 11008067]
38. Yoshioka K, Saitoh O, Nakata H. Heteromeric association creates a P2Y-like adenosine receptor. *Proc Natl Acad Sci U S A*. 2001; 98:7617–7622. [PubMed: 11390975]
39. Yegutkin GG. Nucleotide- and nucleoside-converting ectoenzymes: Important modulators of purinergic signalling cascade. *Biochim Biophys Acta*. 2008; 1782:673–694. [PubMed: 18302942]
40. Elliott MR, Chekeni FB, Trampont PC, Lazarowski ER, Kadl A, Walk SF, Park RI, Woodson D, Ostankovich M, Sharma P, Lysiak JJ, Harden TK, Leitinger N, Ravichandran KS. Nucleotides released by apoptotic cells act as a find-me signal to promote phagocytic clearance. *Nature*. 2009; 461:181–182. [PubMed: 19741694]
41. Relvas LJ, Bouffieux C, Marcet B, Communi D, Makhoul M, Horckmans M, Blero C, Bruyins D, Caspers L, Boeynaems JM, Willermann F. Extracellular nucleotides and interleukin-8 production by ARPE cells: potential role of danger signals in blood-retinal barrier activation. *Invest Ophthalmol Vis Sci*. 2009; 50:1241–1246. [PubMed: 19029040]
42. Junger WG, Hoyt DB, Davis RE, Herdon-Remelius C, Namiki S, Junger H, Loomis W, Altman A. Hypertonicity regulates the function of human neutrophils by modulating chemoattractant receptor

signaling and activating mitogen-activated protein kinase p38. *J Clin Invest.* 1998; 101:2768–2779. [PubMed: 9637711]

**Fig. 1.**

ATP release channels in PMNs. **(A)** The abundance of mRNAs for the TTYH1 and TTYH3 maxi-anion channels, connexin 43 (Cx 43), and pannexin-1 (Panx 1) in human brain, primary human PMNs, and HL-60 cells, before and after differentiation (dHL-60) with 1.3% DMSO for 3 days, were estimated by real-time RT-PCR. nt, not tested; nd, not detected. Values are expressed as the mean \pm SD, and data are representative of four experiments. **(B)** Immunostaining of primary human PMNs with antibodies against TTYH1, TTYH3, and Cx 43. **(C)** Immunostaining of Panx 1 on primary human PMNs that were either unstimulated or were stimulated with fMLP (1 nM). **(D)** Colocalization of F-actin (red), Panx 1 (green), and FPR (blue) in unpolarized human PMNs and in PMNs that were polarized by stimulation

with fMLP (1 nM) that was added uniformly for 10 min. The images shown in panels B and D are representative of experiments performed at least twice with cells from different donors; panel C is representative of at least 3 separate experiments.

**Fig. 2.**

Maxi-anion and Panx 1 channels mediate the FPR-induced release of ATP from PMNs. (**A** and **B**) The effects of DIDS, CBX, 10 Panx 1, or a nonsense control peptide on the release of ATP from human PMNs in response to FPR stimulation with 100 nM fMLP for 3 min were examined. (**C** to **E**) The effects of DIDS, CBX, 10 Panx 1, or nonsense control peptide on the functional responses of human PMNs stimulated with fMLP were determined. (**F**) Effect of knocking down TTYH3 on ATP release and oxidative burst of dHL-60 cells in response to fMLP. Values in all panels are expressed as the mean \pm SD and data are representative of individual experiments with cells from different donors (n donors), Student's t-test, *, $P < 0.05$.

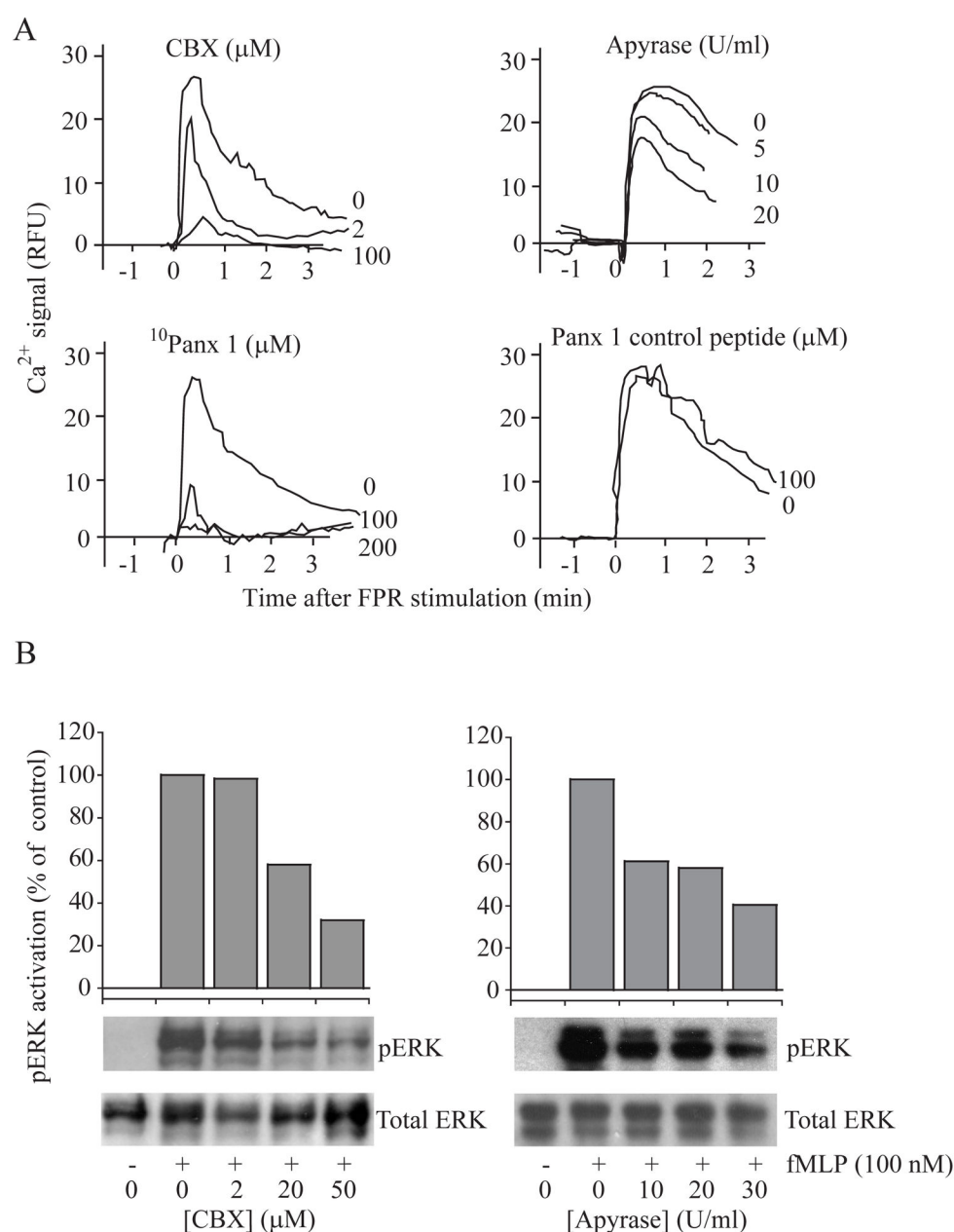
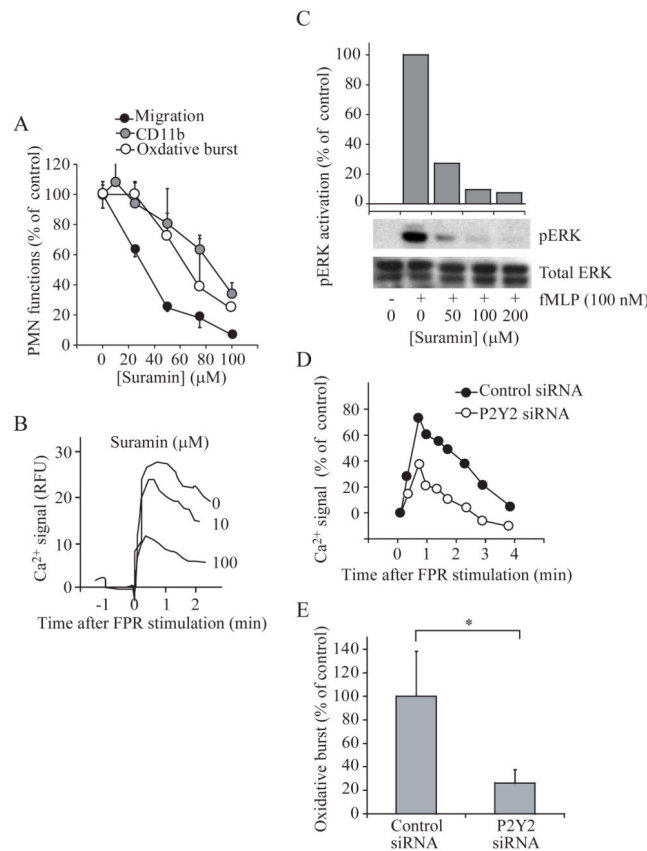
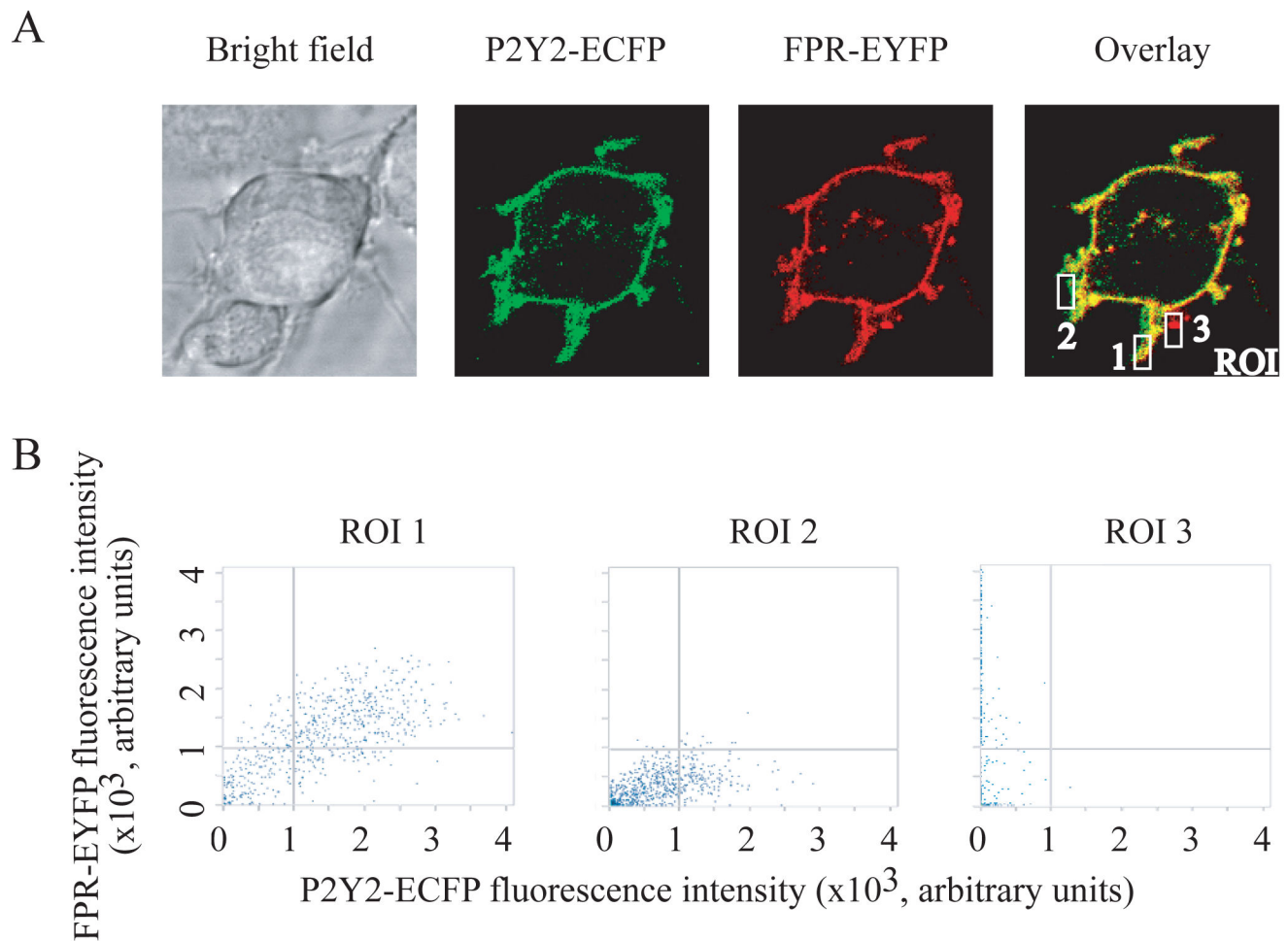


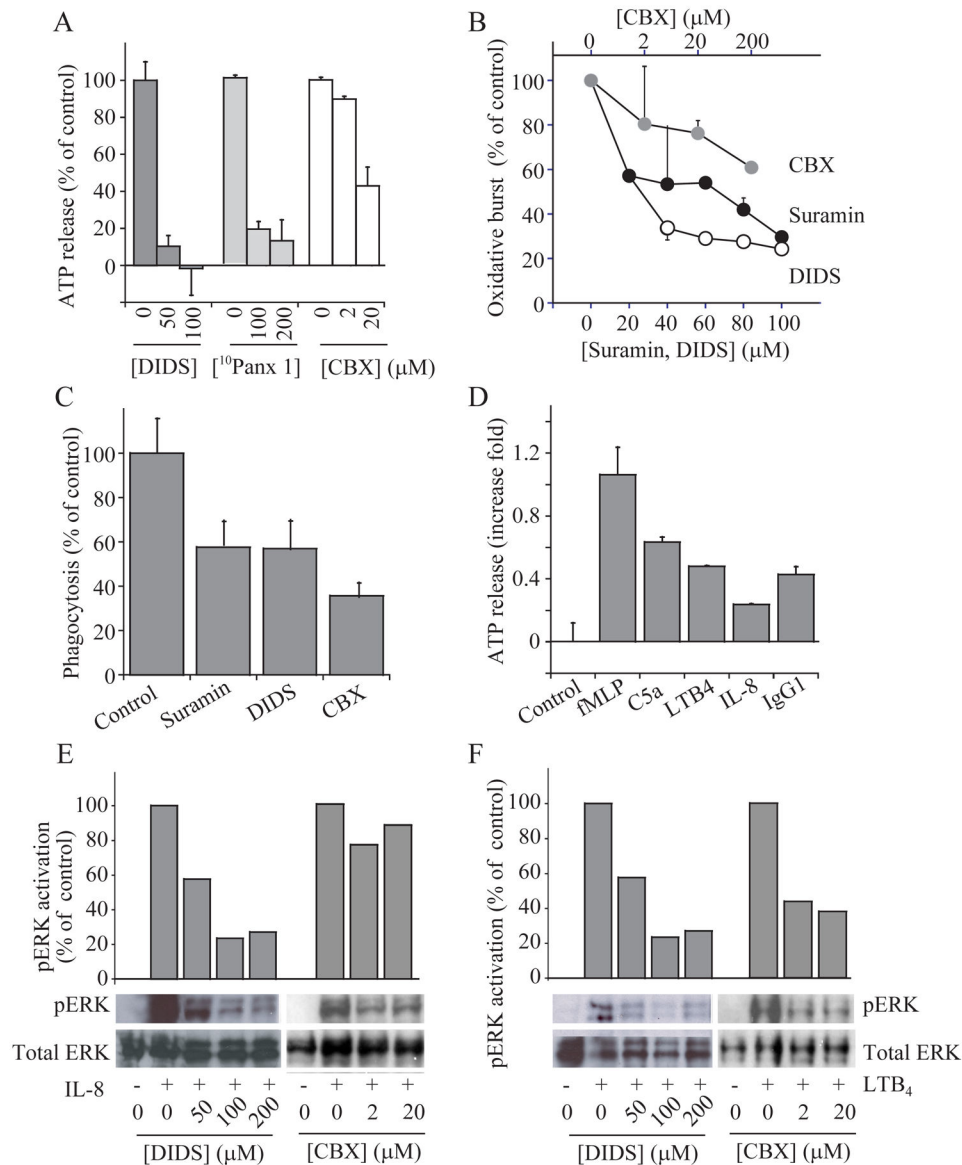
Fig. 3. FPR-induced Ca^{2+} mobilization and MAPK activation in human PMNs require the release of ATP. **(A)** Intracellular Ca^{2+} mobilization in response to fMLP (10 nM) in human PMNs pretreated with the indicated concentrations of apyrase, CBX or $^{10}\text{Panx 1}$. Data are expressed as relative fluorescence units (RFU). **(B)** Effect of pretreatment of human PMNs with the indicated concentrations of CBX or apyrase on fMLP-stimulated activation of ERK, which was determined by assessing the ratio of the abundance of phosphorylated ERK (pERK) to that of total ERK protein. The data are representative of individual experiments with cells from different donors ($n = 4$ in panel A and 3 in panel B).

**Fig. 4.**

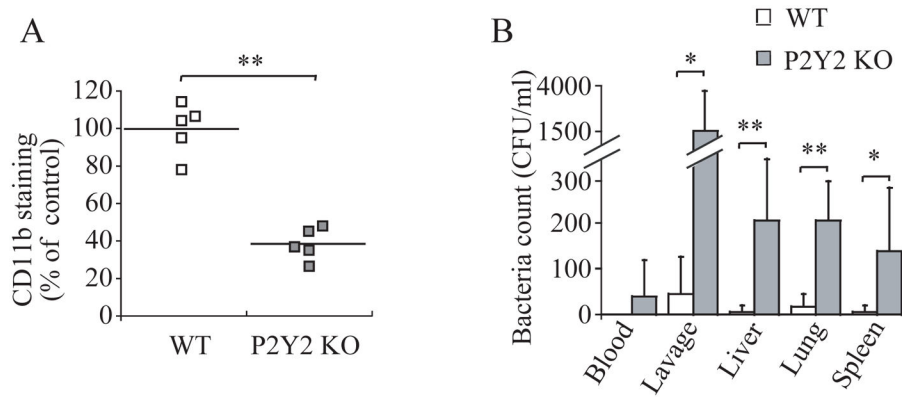
P2 purinergic receptors are required for FPR-induced cellular responses in human PMNs. (A) The effects of the P2 receptor antagonist suramin on the functional responses of human PMNs to fMLP were examined. (B) The effect of suramin on Ca^{2+} signaling in PMNs in response to fMLP was examined. (C) The effect of suramin on fMLP-induced activation of ERK in PMNs was determined. (D and E) The effect of knockdown of P2Y2 receptors in dHL-60 cells on FPR-induced Ca^{2+} signaling and oxidative burst, which was assessed by flow cytometric analysis of Fluo-3 and DHR, respectively, was examined. Data are expressed as a percentage of controls treated with nonsense siRNA. Values are expressed as mean \pm SD (A and E) and the data are representative of at least three individual experiments with similar results. *, $P < 0.05$.

**Fig. 5.**

FPR and P2Y2 receptors colocalize on the cell surface. **(A)** dHL-60 cells were cotransfected with plasmids encoding P2Y2-ECFP and FPR-EYFP, and receptor distribution was assessed by confocal laser scanning microscopy. **(B)** The degree of receptor colocalization in different regions of interest (ROI) was evaluated by regression analysis. ROI 1, ROI 2, and ROI 3 indicate areas with different degrees of receptor colocalization shown in the right-most image in (A). The data are representative of more than three individual experiments.

**Fig. 6.**

ATP release and autocrine feedback through purinergic receptors are a general requirement for the activation of PMNs. (**A** and **B**) Effects of DIDS, suramin, and CBX on ATP release and oxidative burst in human PMNs stimulated by ligation of $\text{Fc}\gamma$ receptors with IgG₁ antibodies (5 $\mu\text{g}/\text{ml}$). (**C**) Effects of DIDS (100 μM), suramin (100 μM), and CBX (20 μM) on the phagocytosis of opsonized bacteria by human PMNs. (**D**) ATP release by human PMNs stimulated with fMLP (100 nM, 3 min), C5a (10 ng/ml, 2 min), LTB₄ (10 nM, 1 min), IL-8 (10 ng/ml, 2 min), or IgG₁ (5 $\mu\text{g}/\text{ml}$, 10 min). Values are expressed as the mean \pm SD. (**E** and **F**) Effects of DIDS or CBX on the activation of ERK in human PMNs that were stimulated with IL-8 (10 ng/ml, 2 min) or LTB₄ (10 nM, 1 min). The data are representative of individual experiments with cells from at least three different donors.

**Fig. 7.**

P2Y2 receptors are required for immune defense in a mouse model of peritoneal infection.

(A) Production of CD11b in PMNs from wild-type (WT) controls and P2Y2 receptor knockout mice (P2Y2 KO). The abundance of CD11b on Gr-1-positive PMNs was determined 2 hours after induction of infection by cecal ligation and puncture (CLP; $n = 5$ mice in each group). (B) Bacterial concentrations expressed as colony forming units per ml (CFU/ml) in peripheral blood, peritoneal lavage fluid, and extracts from liver, lung, and spleen of WT or P2Y2 KO mice were determined 3 hours after CLP ($n = 6$ mice in each group). Data are expressed as the mean \pm SD. *, $P < 0.05$; **, $P < 0.001$.